

A WEAK GALERKIN METHOD FOR ELASTICITY INTERFACE PROBLEMS

CHUNMEI WANG * AND SHANGYOU ZHANG[†]

Abstract. This article introduces a weak Galerkin (WG) finite element method for linear elasticity interface problems on general polygonal/polyhedra partitions. The developed WG method has been proved to be stable and accurate with optimal order error estimates in the discrete H^1 norm. Some numerical experiments are conducted to verify the efficiency and accuracy of the proposed WG method.

Key words. weak Galerkin, WG, finite element methods, elasticity interface problems, polygonal or polyhedral partition.

AMS subject classifications. Primary, 65N30, 65N15, 65N12, 74N20; Secondary, 35B45, 35J50, 35J35

1. Introduction. In this paper we are concerned with the development of weak Galerkin (WG) finite element methods for elasticity interface problems. To this end, assume $\Omega \subset \mathbb{R}^d$ ($d = 2, 3$) is an open bounded domain with piecewise smooth Lipschitz boundary $\partial\Omega$. Let N and M be two positive integers. The domain Ω is partitioned into a set of subdomains $\{\Omega_i\}_{i=1}^N$ with piecewise smooth Lipschitz boundary $\partial\Omega_i$ for $i = 1, \dots, N$; $\Gamma = \bigcup_{i=1}^N \partial\Omega_i \setminus \partial\Omega$ is the interface between the subdomains in the sense that

$$\Gamma = \bigcup_{m=1}^M \Gamma_m,$$

where there exist $i, j \in \{1, \dots, N\}$ such that $\Gamma_m = \partial\Omega_i \cap \partial\Omega_j$ for $m = 1, \dots, M$. We consider the following elasticity interface problem: Find the displacement \mathbf{u} such that

$$(1.1) \quad \begin{aligned} \boldsymbol{\sigma}(\mathbf{u}_i) &= 2\mu_i \boldsymbol{\epsilon}(\mathbf{u}_i) + \lambda_i \nabla \cdot \mathbf{u}_i I, & \text{in } \Omega_i, i = 1, \dots, N, \\ -\nabla \cdot \boldsymbol{\sigma}(\mathbf{u}_i) &= \mathbf{f}_i, & \text{in } \Omega_i, i = 1, \dots, N, \\ \llbracket \mathbf{u} \rrbracket_{\Gamma_m} &= \phi_m, & \text{on } \Gamma_m, m = 1, \dots, M, \\ \llbracket \boldsymbol{\sigma}(\mathbf{u}) \mathbf{n} \rrbracket_{\Gamma_m} &= \boldsymbol{\psi}_m, & \text{on } \Gamma_m, m = 1, \dots, M, \\ \mathbf{u}_i &= \mathbf{g}_i, & \text{on } \partial\Omega_i \cap \partial\Omega, i = 1, \dots, N, \end{aligned}$$

where $\mathbf{u}_i = \mathbf{u}|_{\Omega_i}$, $\mathbf{f}_i = \mathbf{f}|_{\Omega_i}$, $\mathbf{g}_i = \mathbf{g}|_{\Omega_i}$, $\mu_i = \mu|_{\Omega_i}$, $\lambda_i = \lambda|_{\Omega_i}$, $\llbracket \boldsymbol{\sigma}(\mathbf{u}) \mathbf{n} \rrbracket_{\Gamma_m} = \boldsymbol{\sigma}(\mathbf{u}_i) \mathbf{n}_i + \boldsymbol{\sigma}(\mathbf{u}_j) \mathbf{n}_j$ with \mathbf{n}_i and \mathbf{n}_j being the unit outward normal directions to $\partial\Omega_i \cap \Gamma_m$ and $\partial\Omega_j \cap \Gamma_m$, and $\llbracket \mathbf{u} \rrbracket_{\Gamma_m} = \mathbf{u}_i|_{\Gamma_m} - \mathbf{u}_j|_{\Gamma_m}$. Throughout this paper, we use bold face letters to denote vector valued functions and their associated function spaces. Here, $\boldsymbol{\epsilon} = \frac{1}{2}(\nabla \mathbf{u} + \nabla \mathbf{u}^T)$ is the strain tensor; \mathbf{f} represents a given body force; and λ and

*Department of Mathematics, University of Florida, Gainesville, FL 32611, USA (chunmei.wang@ufl.edu). The research of Chunmei Wang was partially supported by National Science Foundation Award DMS-2136380.

[†]Department of Mathematical Sciences, University of Delaware, Newark, DE 19716, USA (szhang@udel.edu).

μ are the positive Lamé parameters. Regarding to the Young's modulus E , and the Poisson's ratio ν , the following identities hold true; i.e.,

$$\lambda = \frac{E\nu}{(1-2\nu)(1+\nu)}, \quad \mu = \frac{E}{2(1+\nu)}.$$

The Lamé parameters λ and μ are assumed to be piecewise smooth functions with respect to the partition $\Omega = \bigcup_{i=1}^N \Omega_i$. We assume that $\frac{\lambda}{\mu} = \frac{2\nu}{1-2\nu}$ is bounded.

Elasticity interface problems play an important role in continuum mechanics where the elasticity theory and the governing partial differential equations (PDEs) describe various material behaviors. An interface description for this class of problem in the elasticity theory is indispensable whenever there are voids, pores, inclusions, dislocations, cracks or composite structures in materials [5, 7, 17, 19]. In particular, the elasticity interface problems are crucial in tissue engineering, biomedical science and biophysics [21, 22, 28]. In many situations, the interface is not static such as fluid–structure interfacial boundaries [26]. Discontinuities in material properties often occur over the interface. When an elastic body is occupied by heterogeneous materials with distinct physical parameters, the governing equation holds on each disjoint domain. The solution to the governing equation is required to satisfy the displacement and traction jump conditions along the interface between different materials besides the usual boundary conditions. In the linear elasticity theory, the stress–strain relation is governed by the constitutive equations. For the isotropic homogeneous materials, constitutive equations are determined by any two terms of bulk modulus, Young's modulus, Lamé's first parameter, shear modulus, Poisson's ratio, and P-wave modulus [2]. For these moduli being position dependent functions, the related constitutive equations describe elasticity property of isotropic inhomogeneous media. In seismic wave equations, inhomogeneity is accounted by assuming Lamé's parameters to be a position dependent function [18].

Many numerical methods have been designed for elasticity interface problems. The immersed interface method (IIM) [13] was proposed to solve elasticity interface problems for isotropic homogeneous media [29, 6]. A second-order sharp numerical method was developed for linear elasticity equations [20]. Finite element methods including the partition of unity method (PUM), the generalized finite element method (GFEM) and the extended finite element method (XFEM) were developed to capture the non-smooth property of the solution over the interface by adding enrichment functions to the approximation [7, 17, 19]. The discontinuous Galerkin finite element methods were employed to simulate strong and weak discontinuities [8, 3, 14] through the weak enforcement of the continuity. The immersed finite element method (IFM) was proposed to solve elasticity problems with inhomogeneous jump conditions [11, 27, 4]. The sharp-edged interface was proposed for a special elasticity interface problem [9]. The bilinear IFM was introduced and further modified to a locking-free version [12, 10]. The immersed meshfree Galerkin method was proposed for composite solids [23]. A Nitsche type method was proposed for elasticity interface problems [15].

The weak formulation for the elasticity interface model problem (1.1) is as follows: Find \mathbf{u} satisfying $\mathbf{u}_i = \mathbf{g}_i$ on $\partial\Omega_i \cap \partial\Omega$ ($i = 1, \dots, N$), such that

$$(1.2) \quad (2\mu\epsilon(\mathbf{u}), \epsilon(\mathbf{v})) + (\lambda\nabla \cdot \mathbf{u}, \nabla \cdot \mathbf{v}) = (\mathbf{f}, \mathbf{v}) + \sum_{m=1}^M \langle \boldsymbol{\psi}, \mathbf{v} \rangle_{\Gamma_m}, \quad \forall \mathbf{v} \in [H_0^1(\Omega)]^d.$$

We follow the standard notations for Sobolev spaces and norms defined on a given open and bounded domain $D \subset \mathbb{R}^d$ with Lipschitz continuous boundary. As such, $\|\cdot\|_{s,D}$ and $|\cdot|_{s,D}$ are used to denote the norm and seminorm in the Sobolev space $H^s(D)$ for any $s \geq 0$. The inner product in $H^s(D)$ is denoted by $(\cdot, \cdot)_{s,D}$ for $s \geq 0$. The space $H^0(D)$ coincides with $L^2(D)$ (i.e., the space of square integrable functions), for which the norm and the inner product are denoted as $\|\cdot\|_D$ and $(\cdot, \cdot)_D$. When $D = \Omega$ or when the domain of integration is clear from the context, we shall drop the subscript D in the norm and the inner product notation.

The paper is organized as follows. In Section 2, we briefly review the weak differential operators and their discrete analogies. In Section 3, the WG method for the model problem (1.1) based on the weak formulation (1.2) is proposed. In Section 4, we establish the solution existence, uniqueness, and stability. In Section 5, we derive an error equation for the WG solutions. The optimal order error estimate for the exact solution in the discrete H^1 norm is established in Section 6. Finally, a couple of numerical results to illustrate and verify our convergence theory are reported in Section 7.

2. Weak Differential Operators. The two principal differential operators in the weak formulation (1.2) for the elasticity interface model problem (1.1) are the divergence operator $(\nabla \cdot)$ and the gradient operator ∇ . The discrete weak versions for $(\nabla \cdot)$ and ∇ have been introduced in [24, 25]. For completeness, we shall briefly review their definitions in this section.

Let T be a polygonal or polyhedral domain with boundary ∂T . A vector-valued weak function on T refers to $\mathbf{v} = \{\mathbf{v}_0, \mathbf{v}_b\}$ with $\mathbf{v}_0 \in [L^2(T)]^d$ and $\mathbf{v}_b \in [L^2(\partial T)]^d$. Here \mathbf{v}_0 and \mathbf{v}_b are used to represent the values of \mathbf{v} in the interior and on the boundary of T respectively. Note that \mathbf{v}_b may not necessarily be the trace of \mathbf{v}_0 on ∂T . Denote by $\mathcal{W}(T)$ the space of weak functions on T ; i.e.,

$$(2.1) \quad \mathcal{W}(T) = \{\mathbf{v} = \{\mathbf{v}_0, \mathbf{v}_b\} : \mathbf{v}_0 \in [L^2(T)]^d, \mathbf{v}_b \in [L^2(\partial T)]^d\}.$$

The weak divergence of $\mathbf{v} \in \mathcal{W}(T)$, denoted by $\nabla_w \cdot \mathbf{v}$, is defined as a linear functional on $H^1(T)$ such that

$$(\nabla_w \cdot \mathbf{v}, w)_T = -(\mathbf{v}_0, \nabla w)_T + \langle \mathbf{v}_b, w \mathbf{n} \rangle_{\partial T},$$

for all $w \in H^1(T)$, where \mathbf{n} is a unit outward normal direction to ∂T .

The weak gradient of $\mathbf{v} \in \mathcal{W}(T)$, denoted by $\nabla_w \mathbf{v}$, is defined as a linear functional on $[H^1(T)]^{d \times d}$ such that

$$(\nabla_w \mathbf{v}, \mathbf{w})_T = -(\mathbf{v}_0, \nabla \cdot \mathbf{w})_T + \langle \mathbf{v}_b, \mathbf{w} \mathbf{n} \rangle_{\partial T},$$

for all $\mathbf{w} \in [H^1(T)]^{d \times d}$.

Denote by $P_r(T)$ the space of polynomials on T with degree no more than r . A discrete version of $\nabla_w \cdot \mathbf{v}$ for $\mathbf{v} \in \mathcal{W}(T)$, denoted by $\nabla_{w,r,T} \cdot \mathbf{v}$, is defined as the unique polynomial in $P_r(T)$ satisfying

$$(2.2) \quad (\nabla_{w,r,T} \cdot \mathbf{v}, w)_T = -(\mathbf{v}_0, \nabla w)_T + \langle \mathbf{v}_b, w \mathbf{n} \rangle_{\partial T}, \quad \forall w \in P_r(T).$$

A discrete version of $\nabla_w \mathbf{v}$ for $\mathbf{v} \in \mathcal{W}(T)$, denoted by $\nabla_{w,r,T} \mathbf{v}$, is defined as a unique polynomial matrix in $[P_r(T)]^{d \times d}$ satisfying

$$(2.3) \quad (\nabla_{w,r,T} \mathbf{v}, \mathbf{w})_T = -(\mathbf{v}_0, \nabla \cdot \mathbf{w})_T + \langle \mathbf{v}_b, \mathbf{w} \mathbf{n} \rangle_{\partial T}, \quad \forall \mathbf{w} \in [P_r(T)]^{d \times d}.$$

Using the weak gradient, we define the weak strain tensor as follows:

$$\epsilon_w(\mathbf{v}) = \frac{1}{2}(\nabla_w \mathbf{v} + \nabla_w \mathbf{v}^T).$$

A discrete version of $\epsilon_w(\mathbf{v})$ for $\mathbf{v} \in \mathcal{W}(T)$, denoted by $\epsilon_{w,r,T}(\mathbf{v})$, is defined as a unique polynomial matrix in $[P_r(T)]^{d \times d}$ satisfying

$$(2.4) \quad (\epsilon_{w,r,T}(\mathbf{v}), \mathbf{w})_T = -(\mathbf{v}_0, \epsilon(\mathbf{w}))_T + \langle \mathbf{v}_b, \mathbf{w}\mathbf{n} \rangle_{\partial T},$$

for any symmetric matrix $\mathbf{w} \in [P_r(T)]^{d \times d}$.

3. Weak Galerkin Algorithm. Let \mathcal{T}_h be a finite element partition of the domain Ω consisting of polygons or polyhedra that are shape-regular [25]. Assume that the edges/faces of the elements in \mathcal{T}_h align with the interface Γ . The partition \mathcal{T}_h can be grouped into N sets of elements denoted by $\mathcal{T}_h^i = \mathcal{T}_h \cap \Omega_i$, so that each \mathcal{T}_h^i provides a finite element partition for the subdomain Ω_i for $i = 1, \dots, N$. The intersection of the partition \mathcal{T}_h also introduces a finite element partition for the interface Γ , denoted by Γ_h . Denote by \mathcal{E}_h the set of all edges or flat faces in \mathcal{T}_h and $\mathcal{E}_h^0 = \mathcal{E}_h \setminus \partial\Omega$ the set of all interior edges or flat faces. Denote by h_T the meshsize of $T \in \mathcal{T}_h$ and $h = \max_{T \in \mathcal{T}_h} h_T$ the meshsize for the partition \mathcal{T}_h .

On each element $T \in \mathcal{T}_h$, denote by $RM(T)$ the space of rigid motions on T given by

$$RM(T) = \{\mathbf{a} + \eta \mathbf{x} : \mathbf{a} \in \mathbb{R}^d, \eta \in so(d)\},$$

where \mathbf{x} is the position vector on T and $so(d)$ is the space of skew-symmetric $d \times d$ matrices. The trace of the rigid motion on each edge $e \subset T$ forms a finite dimensional space denoted by $P_{RM}(e)$; i.e.,

$$P_{RM}(e) = \{\mathbf{v} \in [L^2(e)]^d : \mathbf{v} = \tilde{\mathbf{v}}|_e \text{ for some } \tilde{\mathbf{v}} \in RM(T), e \subset \partial T\}.$$

For any integer $k \geq 1$, denote by $W_k(T)$ the local discrete space of the weak functions given by

$$W_k(T) = \{\{\mathbf{v}_0, \mathbf{v}_b\} : \mathbf{v}_0 \in [P_k(T)]^d, \mathbf{v}_b \in S_k(e), e \subset \partial T\},$$

where $S_k(e) = [P_{k-1}(e)]^d + P_{RM}(e)$. Since $P_{RM}(e) \subset P_1(e)$, then the boundary component $S_k(e)$ is given by $[P_{k-1}(e)]^d$ for $k > 1$ and $P_{RM}(e)$ for $k = 1$.

Patching $W_k(T)$ over all the elements $T \in \mathcal{T}_h$ through a common value \mathbf{v}_b on the interior interface \mathcal{E}_h^0 (excluding the interface Γ), we arrive at the following weak finite element space W_h ; i.e.,

$$W_h = \{\{\mathbf{v}_0, \mathbf{v}_b\} : \{\mathbf{v}_0, \mathbf{v}_b\}|_T \in W_k(T), \forall T \in \mathcal{T}_h\}.$$

Denote by W_h^0 the subspace of W_h with homogeneous boundary values; i.e.,

$$W_h^0 = \{\{\mathbf{v}_0, \mathbf{v}_b\} \in W_h : \mathbf{v}_b|_{\partial\Omega} = 0\}.$$

For simplicity of notation and without confusion, for any $\mathbf{v} \in W_h$, denote by $\nabla_w \cdot \mathbf{v}$, $\nabla_w \mathbf{v}$ and $\epsilon_w(\mathbf{v})$ the discrete weak actions $\nabla_{w,k-1,T} \cdot \mathbf{v}$, $\nabla_{w,k-1,T} \mathbf{v}$ and $\epsilon_{w,k-1,T}(\mathbf{v})$ computed by using (2.2), (2.3) and (2.4) on each element T respectively; i.e.,

$$\nabla_w \cdot \mathbf{v}|_T = \nabla_{w,k-1,T} \cdot (\mathbf{v}|_T), \quad \mathbf{v} \in W_h,$$

$$(\nabla_w \mathbf{v})|_T = \nabla_{w,k-1,T}(\mathbf{v}|_T), \quad \mathbf{v} \in W_h,$$

$$(\epsilon_{w,r,T}(\mathbf{v}))|_T = \epsilon_{w,k-1,T}(\mathbf{v}|_T), \quad \mathbf{v} \in W_h.$$

Denote by \mathbf{Q}_b the L^2 projection onto the space $S_k(e)$. For any $\mathbf{u}, \mathbf{v} \in W_h$, we introduce the following bilinear forms

$$(3.1) \quad s(\mathbf{u}, \mathbf{v}) = \sum_{T \in \mathcal{T}_h} s_T(\mathbf{u}, \mathbf{v}),$$

$$(3.2) \quad a(\mathbf{u}, \mathbf{v}) = \sum_{T \in \mathcal{T}_h} a_T(\mathbf{u}, \mathbf{v}),$$

where

$$\begin{aligned} s_T(\mathbf{u}, \mathbf{v}) &= h_T^{-1} \langle \mathbf{Q}_b \mathbf{u}_0 - \mathbf{u}_b, \mathbf{Q}_b \mathbf{v}_0 - \mathbf{v}_b \rangle_{\partial T}, \\ a_T(\mathbf{u}, \mathbf{v}) &= (2\mu \epsilon_w(\mathbf{u}), \epsilon_w(\mathbf{v}))_T + (\lambda \nabla_w \cdot \mathbf{u}, \nabla_w \cdot \mathbf{v})_T. \end{aligned}$$

The following is the weak Galerkin scheme for the elasticity interface problem (1.1) based on the variational formulation (1.2).

WEAK GALERKIN ALGORITHM 3.1. Find $\mathbf{u}_h \in W_h$, such that $\mathbf{u}_b = \mathbf{Q}_b \mathbf{g}_i$ on $\partial\Omega_i \cap \partial\Omega$ for $i = 1, \dots, N$ and $\mathbf{u}_b^L - \mathbf{u}_b^R = \mathbf{Q}_b \phi_m$ on Γ_m for $m = 1, \dots, M$, s.t.

$$(3.3) \quad s(\mathbf{u}, \mathbf{v}) + a(\mathbf{u}, \mathbf{v}) = (\mathbf{f}, \mathbf{v}_0) + \sum_{m=1}^M \langle \boldsymbol{\psi}, \mathbf{v}_b \rangle_{\Gamma_m},$$

for any $\mathbf{v} \in W_h^0$. Here \mathbf{u}_b^L and \mathbf{u}_b^R denote $\mathbf{u}_b|_{\Omega_i}$ and $\mathbf{u}_b|_{\Omega_j}$ if $\Gamma = \partial\Omega_i \cap \partial\Omega_j$ for some i and j .

4. Stability Analysis. LEMMA 4.1. [24] (Second Korn's Inequality) Assume that the domain Ω is connected, open bounded with Lipschitz continuous boundary. Let $\Xi \subset \partial\Omega$ be a nontrivial portion of the boundary $\partial\Omega$ with dimension $d-1$. For any fixed real number $1 \leq p < \infty$, there exists a constant C such that

$$(4.1) \quad \|\mathbf{v}\|_1 \leq C(\|\epsilon(\mathbf{v})\|_0 + \|\mathbf{v}\|_{L^p(\Xi)}),$$

for any $\mathbf{v} \in [H^1(\Omega)]^d$.

THEOREM 4.2. There exists a unique solution to the weak Galerkin finite element scheme (3.3).

Proof. Since the number of equations is equal to the number of unknowns in (3.3), it suffices to prove the solution uniqueness. To this end, let $\mathbf{u}_h^{(1)} = \{\mathbf{u}_0^{(1)}, \mathbf{u}_b^{(1)}\}$ and $\mathbf{u}_h^{(2)} = \{\mathbf{u}_0^{(2)}, \mathbf{u}_b^{(2)}\} \in W_h$ be two different solutions of (3.3). It follows that $\mathbf{u}_b^{(j)}$ ($j = 1, 2$) satisfies $\mathbf{u}_b^{(j)} = \mathbf{Q}_b \mathbf{g}_i$ on $\partial\Omega_i \cap \partial\Omega$ for $i = 1, \dots, N$ and $\mathbf{u}_b^{(j),L} - \mathbf{u}_b^{(j),R} = \mathbf{Q}_b \phi_m$ on Γ_m for $m = 1, \dots, M$, and

$$(4.2) \quad s(\mathbf{u}^{(j)}, \mathbf{v}) + a(\mathbf{u}^{(j)}, \mathbf{v}) = (\mathbf{f}, \mathbf{v}_0) + \sum_{m=1}^M \langle \boldsymbol{\psi}, \mathbf{v}_b \rangle_{\Gamma_m}, \quad \forall \mathbf{v} = \{\mathbf{v}_0, \mathbf{v}_b\} \in W_h^0, j = 1, 2.$$

The difference of the two solutions $\mathbf{w} = \mathbf{u}_h^{(1)} - \mathbf{u}_h^{(2)} \in V_h^0$ satisfies

$$(4.3) \quad s(\mathbf{w}, \mathbf{v}) + a(\mathbf{w}, \mathbf{v}) = 0, \quad \forall \mathbf{v} = \{\mathbf{v}_0, \mathbf{v}_b\} \in W_h^0.$$

This implies that

$$(4.4) \quad \epsilon_w(\mathbf{w}) = 0, \quad \text{in each } T \in \mathcal{T}_h,$$

$$(4.5) \quad \nabla_w \cdot \mathbf{w} = 0, \quad \text{in each } T \in \mathcal{T}_h,$$

$$(4.6) \quad \mathbf{Q}_b \mathbf{w}_0 = \mathbf{w}_b, \quad \text{on each } \partial T.$$

Using (2.3) and the usual integration by parts, we get

$$\begin{aligned} (\nabla_w \mathbf{w}, \mathbf{q})_T &= -(\mathbf{w}_0, \nabla \cdot \mathbf{q})_T + \langle \mathbf{w}_b, \mathbf{q}\mathbf{n} \rangle_{\partial T} \\ &= (\nabla \mathbf{w}_0, \mathbf{q})_T - \langle \mathbf{w}_0 - \mathbf{w}_b, \mathbf{q}\mathbf{n} \rangle_{\partial T} \\ &= (\nabla \mathbf{w}_0, \mathbf{q})_T - \langle \mathbf{Q}_b \mathbf{w}_0 - \mathbf{w}_b, \mathbf{q}\mathbf{n} \rangle_{\partial T}, \end{aligned}$$

for any $\mathbf{q} \in [P_{k-1}(T)]^{d \times d}$. Using (4.6) gives $\nabla_w \mathbf{w} = \nabla \mathbf{w}_0$ on each element T . Using (4.4), we have $\epsilon(\mathbf{w}_0) = \epsilon_w(\mathbf{w}) = 0$, which yields $\mathbf{w}_0 \in RM(T) \subset [P_1(T)]^d$. Using $\mathbf{w}_0|_e = \mathbf{Q}_b \mathbf{w}_0 = \mathbf{w}_b$ we obtain \mathbf{w}_0 is a continuous function in Ω with vanishing boundary value on $\partial\Omega$. Using the second Korn's inequality (4.1) gives $\mathbf{w}_0 \equiv 0$ in Ω , and further $\mathbf{w}_b \equiv 0$ due to (4.6). Therefore, we have $\mathbf{u}_h^{(1)} = \mathbf{u}_h^{(2)}$. This completes the proof of the theorem. \square

5. Error Equations. The goal of this section is to derive the error equation for the weak Galerkin method (3.3). The error equation plays a crucial role in the convergence analysis discussed in Section 6.

Let \mathbf{Q}_0 and \mathbf{Q}_b be the L^2 projection operators onto $[P_k(T)]^d$ and $S_k(e)$ respectively. For $\mathbf{w} \in H^1(\Omega)$, define the L^2 projection $\mathbf{Q}_h \mathbf{w} \in W_h$ as follows

$$\mathbf{Q}_h \mathbf{w}|_T = \{\mathbf{Q}_0 \mathbf{w}, \mathbf{Q}_b \mathbf{w}\}.$$

Denote by \mathcal{Q}_h the L^2 projection operator onto the finite element space of piecewise polynomials of degree $k-1$.

For simplicity, we assume the coefficients μ and λ are piecewise constants with respect to the finite element partition \mathcal{T}_h . Note that the analysis can be extended to piecewise smooth coefficients μ and λ without any difficulty.

LEMMA 5.1. [24] *The operators \mathbf{Q}_h and \mathcal{Q}_h satisfy the following commutative properties:*

$$(5.1) \quad \epsilon_w(\mathbf{Q}_h \mathbf{w}) = \mathcal{Q}_h(\epsilon(\mathbf{w})), \quad \forall \mathbf{w} \in [H^1(T)]^d,$$

$$(5.2) \quad \nabla_w \cdot (\mathbf{Q}_h \mathbf{w}) = \mathcal{Q}_h(\nabla \cdot \mathbf{w}), \quad \forall \mathbf{w} \in [H^1(T)]^d.$$

Let \mathbf{u} and $\mathbf{u}_h \in W_h$ be the exact solution of the elasticity interface problem (1.1) and its numerical solution arising from the WG scheme (3.3). Denote the error function by

$$(5.3) \quad \mathbf{e}_h = \mathcal{Q}_h \mathbf{u} - \mathbf{u}_h.$$

LEMMA 5.2. Let \mathbf{u} and $\mathbf{u}_h \in W_h$ be the exact solution of elasticity interface problem (1.1) and its numerical solution arising from the WG scheme (3.3). The error function \mathbf{e}_h defined in (5.3) satisfies the following equation:

$$(5.4) \quad \begin{aligned} & s(\mathbf{e}_h, \mathbf{v}) + a(\mathbf{e}_h, \mathbf{v}) = s(\mathbf{Q}_h \mathbf{u}, \mathbf{v}) \\ & - \sum_{T \in \mathcal{T}_h} \langle \mathbf{v}_0 - \mathbf{v}_b, 2\mu(\mathcal{Q}_h(\epsilon(\mathbf{u})) - \epsilon(\mathbf{u})) \cdot \mathbf{n} + \lambda(\mathcal{Q}_h(\nabla \cdot \mathbf{u}) - \nabla \cdot \mathbf{u}) \cdot \mathbf{n} \rangle_{\partial T}. \end{aligned}$$

Proof. Using (2.4), (5.1) and the usual integration by parts gives

$$\begin{aligned} & \sum_{T \in \mathcal{T}_h} (2\mu\epsilon_w(\mathbf{Q}_h \mathbf{u}), \epsilon_w(\mathbf{v}))_T \\ &= \sum_{T \in \mathcal{T}_h} (2\mu\mathcal{Q}_h(\epsilon(\mathbf{u})), \epsilon_w(\mathbf{v}))_T \\ &= \sum_{T \in \mathcal{T}_h} -(2\mu\mathbf{v}_0, \epsilon(\mathcal{Q}_h(\epsilon(\mathbf{u}))))_T + \langle 2\mu\mathbf{v}_b, \mathcal{Q}_h(\epsilon(\mathbf{u})) \cdot \mathbf{n} \rangle_{\partial T} \\ &= \sum_{T \in \mathcal{T}_h} (2\mu\epsilon(\mathbf{v}_0), \mathcal{Q}_h(\epsilon(\mathbf{u})))_T - \langle 2\mu(\mathbf{v}_0 - \mathbf{v}_b), \mathcal{Q}_h(\epsilon(\mathbf{u})) \cdot \mathbf{n} \rangle_{\partial T} \\ &= \sum_{T \in \mathcal{T}_h} (2\mu\epsilon(\mathbf{v}_0), \epsilon(\mathbf{u}))_T - \langle 2\mu(\mathbf{v}_0 - \mathbf{v}_b), \mathcal{Q}_h(\epsilon(\mathbf{u})) \cdot \mathbf{n} \rangle_{\partial T} \\ &= \sum_{T \in \mathcal{T}_h} (\mathbf{v}_0, -\nabla \cdot (2\mu\epsilon(\mathbf{u})))_T - \langle 2\mu(\mathbf{v}_0 - \mathbf{v}_b), (\mathcal{Q}_h(\epsilon(\mathbf{u})) - \epsilon(\mathbf{u})) \cdot \mathbf{n} \rangle_{\partial T} \\ & \quad + \sum_{m=1}^M \langle \mathbf{v}_b, \llbracket 2\mu\epsilon(\mathbf{u})\mathbf{n} \rrbracket \rangle_{\Gamma_m}, \end{aligned}$$

where we used $\sum_{T \in \mathcal{T}_h} \langle \mathbf{v}_b, \llbracket 2\mu\epsilon(\mathbf{u})\mathbf{n} \rrbracket \rangle_{\partial T} = \sum_{m=1}^M \langle \mathbf{v}_b, \llbracket 2\mu\epsilon(\mathbf{u})\mathbf{n} \rrbracket \rangle_{\Gamma_m}$ since $\mathbf{v}_b = 0$ on $\partial\Omega$ on the last line.

Using (2.2), (5.2) and the usual integration by parts yields

$$\begin{aligned}
& \sum_{T \in \mathcal{T}_h} (\lambda \nabla_w \cdot (\mathbf{Q}_h \mathbf{u}), \nabla_w \cdot \mathbf{v})_T \\
&= \sum_{T \in \mathcal{T}_h} (\lambda \mathcal{Q}_h(\nabla \cdot \mathbf{u}), \nabla_w \cdot \mathbf{v})_T \\
&= \sum_{T \in \mathcal{T}_h} -(\mathbf{v}_0, \nabla(\lambda \mathcal{Q}_h(\nabla \cdot \mathbf{u})))_T + \langle \mathbf{v}_b, \lambda \mathcal{Q}_h(\nabla \cdot \mathbf{u}) \mathbf{n} \rangle_{\partial T} \\
&= \sum_{T \in \mathcal{T}_h} (\nabla \cdot \mathbf{v}_0, \lambda \mathcal{Q}_h(\nabla \cdot \mathbf{u}))_T - \langle \mathbf{v}_0 - \mathbf{v}_b, \lambda \mathcal{Q}_h(\nabla \cdot \mathbf{u}) \mathbf{n} \rangle_{\partial T} \\
&= \sum_{T \in \mathcal{T}_h} (\nabla \cdot \mathbf{v}_0, \lambda \nabla \cdot \mathbf{u})_T - \langle \mathbf{v}_0 - \mathbf{v}_b, \lambda \mathcal{Q}_h(\nabla \cdot \mathbf{u}) \mathbf{n} \rangle_{\partial T} \\
&= \sum_{T \in \mathcal{T}_h} (\mathbf{v}_0, -\nabla \cdot (\lambda \nabla \cdot \mathbf{u} I))_T + \langle \mathbf{v}_0 - \mathbf{v}_b, \lambda \nabla \cdot \mathbf{u} \mathbf{n} \rangle_{\partial T} \\
&\quad - \langle \mathbf{v}_0 - \mathbf{v}_b, \lambda \mathcal{Q}_h(\nabla \cdot \mathbf{u}) \cdot \mathbf{n} \rangle_{\partial T} + \sum_{m=1}^M \langle \mathbf{v}_b, \llbracket \lambda \nabla \cdot \mathbf{u} \mathbf{n} \rrbracket \rangle_{\Gamma_m} \\
&= \sum_{T \in \mathcal{T}_h} (\mathbf{v}_0, -\nabla \cdot (\lambda \nabla \cdot \mathbf{u} I))_T - \langle \mathbf{v}_0 - \mathbf{v}_b, \lambda (\mathcal{Q}_h(\nabla \cdot \mathbf{u}) - \nabla \cdot \mathbf{u}) \mathbf{n} \rangle_{\partial T} \\
&\quad + \sum_{m=1}^M \langle \mathbf{v}_b, \llbracket \lambda \nabla \cdot \mathbf{u} \mathbf{n} \rrbracket \rangle_{\Gamma_m},
\end{aligned}$$

where we used $\sum_{T \in \mathcal{T}_h} \langle \mathbf{v}_b, \llbracket \lambda \nabla \cdot \mathbf{u} \mathbf{n} \rrbracket \rangle_{\partial T} = \sum_{m=1}^M \langle \mathbf{v}_b, \llbracket \lambda \nabla \cdot \mathbf{u} \mathbf{n} \rrbracket \rangle_{\Gamma_m}$ since $\mathbf{v}_b = 0$ on $\partial\Omega$.

Adding the above two equations gives rise to

$$\begin{aligned}
& s(\mathbf{Q}_h \mathbf{u}, \mathbf{v}) + \sum_{T \in \mathcal{T}_h} (2\mu \epsilon_w(\mathbf{Q}_h \mathbf{u}), \epsilon_w(\mathbf{v}))_T + (\lambda \nabla_w \cdot (\mathbf{Q}_h \mathbf{u}), \nabla_w \cdot \mathbf{v})_T \\
&= s(\mathbf{Q}_h \mathbf{u}, \mathbf{v}) + \sum_{T \in \mathcal{T}_h} (\mathbf{v}_0, -\nabla \cdot (2\mu \epsilon(\mathbf{u})))_T \\
&\quad - \langle 2\mu(\mathbf{v}_0 - \mathbf{v}_b), (\mathcal{Q}_h(\epsilon(\mathbf{u})) - \epsilon(\mathbf{u})) \mathbf{n} \rangle_{\partial T} + (\mathbf{v}_0, -\nabla \cdot (\lambda \nabla \cdot \mathbf{u} I))_T \\
&\quad - \langle \mathbf{v}_0 - \mathbf{v}_b, \lambda (\mathcal{Q}_h(\nabla \cdot \mathbf{u}) - \nabla \cdot \mathbf{u}) \mathbf{n} \rangle_{\partial T} + \sum_{m=1}^M \langle \psi, \mathbf{v}_b \rangle_{\Gamma_m} \\
&= s(\mathbf{Q}_h \mathbf{u}, \mathbf{v}) + (\mathbf{f}, \mathbf{v}_0) + \sum_{m=1}^M \langle \psi, \mathbf{v}_b \rangle_{\Gamma_m} \\
&\quad - \sum_{T \in \mathcal{T}_h} \langle (\mathbf{v}_0 - \mathbf{v}_b), 2\mu(\mathcal{Q}_h(\epsilon(\mathbf{u})) - \epsilon(\mathbf{u})) \mathbf{n} + \lambda(\mathcal{Q}_h(\nabla \cdot \mathbf{u}) - \nabla \cdot \mathbf{u}) \mathbf{n} \rangle_{\partial T}.
\end{aligned}$$

Subtracting (3.3) from the above equation yields (5.4). \square

The equation (5.4) is called the *error equation* for the WG finite element scheme (3.3).

6. Error Estimates. Note that \mathcal{T}_h is a shape-regular finite element partition of the domain Ω . For any $T \in \mathcal{T}_h$ and $\varphi \in H^1(T)$, the following trace inequality holds

true [25]:

$$(6.1) \quad \|\varphi\|_{\partial T}^2 \leq C(h_T^{-1}\|\varphi\|_T^2 + h_T\|\varphi\|_{1,T}^2).$$

If φ is a polynomial, using the inverse inequality, we have

$$(6.2) \quad \|\varphi\|_{\partial T}^2 \leq Ch_T^{-1}\|\varphi\|_T^2.$$

LEMMA 6.1. [25] *Let \mathcal{T}_h be a finite element partition of Ω satisfying the shape regularity assumptions as specified in [25]. The following estimates hold true*

$$(6.3) \quad \sum_{T \in \mathcal{T}_h} h_T^{2l} \|\mathbf{u} - \mathcal{Q}_h \mathbf{u}\|_{l,T}^2 \leq Ch^{2m} \|\mathbf{u}\|_m^2,$$

$$(6.4) \quad \sum_{T \in \mathcal{T}_h} h_T^{2l} \|\mathbf{u} - \mathbf{Q}_0 \mathbf{u}\|_{l,T}^2 \leq Ch^{2(m+1)} \|\mathbf{u}\|_{m+1}^2,$$

$$(6.5) \quad \sum_{T \in \mathcal{T}_h} h_T^{2l} \|\mathbf{u} - \mathbf{Q}_b \mathbf{u}\|_{l,T}^2 \leq Ch^{2m} \|\mathbf{u}\|_m^2,$$

where $0 \leq l \leq 2$ and $0 \leq m \leq k$.

In the weak finite element space W_h , we introduce the following semi-norm

$$\|\mathbf{v}\| = \left(a(\mathbf{v}, \mathbf{v}) + s(\mathbf{v}, \mathbf{v}) \right)^{\frac{1}{2}}.$$

LEMMA 6.2. *There exists a constant C such that*

$$(6.6) \quad \left(\sum_{T \in \mathcal{T}_h} h_T^{-1} \|\mathbf{e}_0 - \mathbf{e}_b\|_{\partial T}^2 \right)^{\frac{1}{2}} \leq C \|\mathbf{e}_h\|.$$

Proof. Using the triangle inequality, the error estimate (6.5) for the projection \mathbf{Q}_b and the trace inequality (6.2), we have

$$(6.7) \quad \begin{aligned} & \left(\sum_{T \in \mathcal{T}_h} h_T^{-1} \|\mathbf{e}_0 - \mathbf{e}_b\|_{\partial T}^2 \right)^{\frac{1}{2}} \\ & \leq \left(\sum_{T \in \mathcal{T}_h} h_T^{-1} \|\mathbf{e}_0 - \mathbf{Q}_b \mathbf{e}_0\|_{\partial T}^2 + h_T^{-1} \|\mathbf{Q}_b \mathbf{e}_0 - \mathbf{e}_b\|_{\partial T}^2 \right)^{\frac{1}{2}} \\ & \leq \left(\sum_{T \in \mathcal{T}_h} h_T^{-2} \|\mathbf{e}_0 - \mathbf{Q}_b \mathbf{e}_0\|_T^2 + h_T^{-1} \|\mathbf{Q}_b \mathbf{e}_0 - \mathbf{e}_b\|_{\partial T}^2 \right)^{\frac{1}{2}} \\ & \leq \left(\sum_{T \in \mathcal{T}_h} |\mathbf{e}_0|_{1,T}^2 + h_T^{-1} \|\mathbf{Q}_b \mathbf{e}_0 - \mathbf{e}_b\|_{\partial T}^2 \right)^{\frac{1}{2}} \\ & \leq C \|\mathbf{e}_h\|. \end{aligned}$$

□

The main convergence result can be stated as follows.

THEOREM 6.3. *Assume $k \geq 1$ and the coefficient coefficients μ and λ are piecewise constants with respect to the finite element partition \mathcal{T}_h . Let \mathbf{u} and $\mathbf{u}_h \in W_h$ be*

the exact solution of the elasticity interface problem (1.1) and its numerical solution arising from the WG scheme (3.3). Assume that \mathbf{u} is sufficiently regular such that $\mathbf{u} \in \prod_{i=1}^N [H^{k+1}(\Omega_i)]^d$. The following error estimate holds true:

$$(6.8) \quad \|\mathbf{e}_h\| \leq Ch^k \left(\sum_{i=1}^N \|\mathbf{u}\|_{k+1, \Omega_i}^2 \right)^{\frac{1}{2}}.$$

Proof. Letting $\mathbf{v} = \mathbf{e}_h$ in (5.4) gives rise to

$$(6.9) \quad \begin{aligned} & s(\mathbf{e}_h, \mathbf{e}_h) + a(\mathbf{e}_h, \mathbf{e}_h) = s(\mathbf{Q}_h \mathbf{u}, \mathbf{e}_h) \\ & - \sum_{T \in \mathcal{T}_h} \langle \mathbf{e}_0 - \mathbf{e}_b, 2\mu(\mathcal{Q}_h(\epsilon(\mathbf{u})) - \epsilon(\mathbf{u})) \cdot \mathbf{n} + \lambda(\mathcal{Q}_h(\nabla \cdot \mathbf{u}) - \nabla \cdot \mathbf{u}) \cdot \mathbf{n} \rangle_{\partial T}. \end{aligned}$$

Using the Cauchy-Schwarz inequality, the trace inequality (6.1) and the estimate (6.4), we have

$$(6.10) \quad \begin{aligned} & s(\mathbf{Q}_h \mathbf{u}, \mathbf{e}_h) \\ & = \sum_{T \in \mathcal{T}_h} \langle \mathbf{Q}_b(\mathbf{Q}_0 \mathbf{u}) - \mathbf{Q}_b \mathbf{u}, \mathbf{Q}_b \mathbf{e}_0 - \mathbf{e}_b \rangle_{\partial T} \\ & \leq \left(\sum_{T \in \mathcal{T}_h} h_T \|\mathbf{Q}_b(\mathbf{Q}_0 \mathbf{u}) - \mathbf{Q}_b \mathbf{u}\|_{\partial T}^2 \right)^{\frac{1}{2}} \left(\sum_{T \in \mathcal{T}_h} h_T^{-1} \|\mathbf{Q}_b \mathbf{e}_0 - \mathbf{e}_b\|_{\partial T}^2 \right)^{\frac{1}{2}} \\ & \leq \left(\sum_{T \in \mathcal{T}_h} h_T \|\mathbf{Q}_0 \mathbf{u} - \mathbf{u}\|_{\partial T}^2 \right)^{\frac{1}{2}} \left(\sum_{T \in \mathcal{T}_h} h_T^{-1} \|\mathbf{Q}_b \mathbf{e}_0 - \mathbf{e}_b\|_{\partial T}^2 \right)^{\frac{1}{2}} \\ & \leq \left(\sum_{T \in \mathcal{T}_h} \|\mathbf{Q}_0 \mathbf{u} - \mathbf{u}\|_T^2 + h_T^2 \|\mathbf{Q}_0 \mathbf{u} - \mathbf{u}\|_{1,T} \right)^{\frac{1}{2}} \\ & \quad \cdot \left(\sum_{T \in \mathcal{T}_h} h_T^{-1} \|\mathbf{Q}_b \mathbf{e}_0 - \mathbf{e}_b\|_{\partial T}^2 \right)^{\frac{1}{2}} \\ & \leq Ch^{k+1} \left(\sum_{i=1}^N \|\mathbf{u}\|_{k+1, \Omega_i}^2 \right)^{\frac{1}{2}} \|\mathbf{e}_h\|. \end{aligned}$$

Using the Cauchy-Schwarz inequality, the trace inequality (6.1), (6.6) and the estimate

(6.3), we have

$$\begin{aligned}
& \sum_{T \in \mathcal{T}_h} \langle \mathbf{e}_0 - \mathbf{e}_b, 2\mu(\mathcal{Q}_h(\epsilon(\mathbf{u})) - \epsilon(\mathbf{u})) \cdot \mathbf{n} + \lambda(\mathcal{Q}_h(\nabla \cdot \mathbf{u}) - \nabla \cdot \mathbf{u}) \cdot \mathbf{n} \rangle_{\partial T} \\
& \leq \sum_{T \in \mathcal{T}_h} \langle \mathbf{e}_0 - \mathbf{e}_b, 2\mu(\mathcal{Q}_h(\epsilon(\mathbf{u})) - \epsilon(\mathbf{u})) \cdot \mathbf{n} + \lambda(\mathcal{Q}_h(\nabla \cdot \mathbf{u}) - \nabla \cdot \mathbf{u}) \cdot \mathbf{n} \rangle_{\partial T} \\
& \leq \left(\sum_{T \in \mathcal{T}_h} h_T^{-1} \|\mathbf{e}_0 - \mathbf{e}_b\|_{\partial T}^2 \right)^{\frac{1}{2}} \\
& \quad \cdot \left(\sum_{T \in \mathcal{T}_h} h_T \|2\mu(\mathcal{Q}_h(\epsilon(\mathbf{u})) - \epsilon(\mathbf{u})) \cdot \mathbf{n} + \lambda(\mathcal{Q}_h(\nabla \cdot \mathbf{u}) - \nabla \cdot \mathbf{u}) \cdot \mathbf{n}\|_{\partial T}^2 \right)^{\frac{1}{2}} \\
(6.11) \quad & \leq \left(\sum_{T \in \mathcal{T}_h} h_T^{-1} \|\mathbf{e}_0 - \mathbf{e}_b\|_{\partial T}^2 \right)^{\frac{1}{2}} \cdot \left\{ \left(\sum_{T \in \mathcal{T}_h} \|2\mu(\mathcal{Q}_h(\epsilon(\mathbf{u})) - \epsilon(\mathbf{u})) \cdot \mathbf{n}\|_T^2 \right. \right. \\
& \quad \left. \left. + h_T^2 \|2\mu(\mathcal{Q}_h(\epsilon(\mathbf{u})) - \epsilon(\mathbf{u})) \cdot \mathbf{n}\|_{1,T}^2 \right)^{\frac{1}{2}} + \left(\sum_{T \in \mathcal{T}_h} \|\lambda(\mathcal{Q}_h(\nabla \cdot \mathbf{u}) - \nabla \cdot \mathbf{u}) \cdot \mathbf{n}\|_T^2 \right. \right. \\
& \quad \left. \left. + h_T^2 \|\lambda(\mathcal{Q}_h(\nabla \cdot \mathbf{u}) - \nabla \cdot \mathbf{u}) \cdot \mathbf{n}\|_{1,T}^2 \right)^{\frac{1}{2}} \right\} \\
& \leq Ch^k \|\mathbf{e}_h\| \left(\sum_{i=1}^N \|\mathbf{u}\|_{k+1, \Omega_i}^2 \right)^{\frac{1}{2}}.
\end{aligned}$$

Substituting (6.10)-(6.11) into (6.9) completes the proof of the theorem. \square

7. Numerical Experiments. In this section, we shall report some numerical results for the weak Galerkin finite element scheme (3.3) proposed and analyzed for elasticity interface problem (1.1) in the previous sections.

In all three test examples, we choose the domain $\Omega = (0, 1)^2$. We solve the following linear elasticity interface problem: Find $\mathbf{u} \in H_0^1(\Omega)^2$ such that

$$(7.1) \quad (2\mu\epsilon(\mathbf{u}), \epsilon(\mathbf{v})) + (\lambda\nabla \cdot \mathbf{u}, \nabla \cdot \mathbf{v}) = (\mathbf{f}, \mathbf{v}) \quad \forall \mathbf{v} \in H_0^1(\Omega)^2.$$

The coefficients are set as, for various positive constants μ_0 and λ_0 ,

$$(7.2) \quad \mu(x, y) = \begin{cases} \frac{\mu_0}{2} & (x, y) \in (\frac{1}{4}, \frac{3}{4})^2, \\ \frac{1}{2} & \text{elsewhere,} \end{cases} \\
\lambda(x, y) = \lambda_0 \mu(x, y).$$

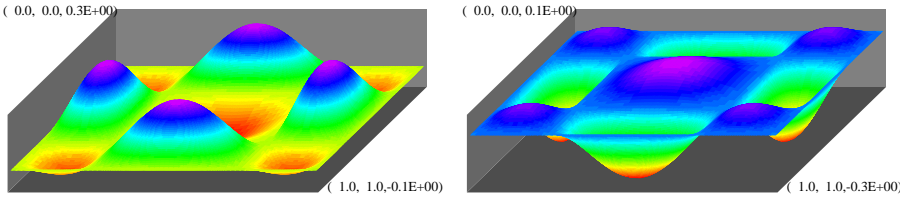


FIG. 7.1. The exact solution \mathbf{u} with $\mu_0 = 10$ and $\lambda_0 = 10$.

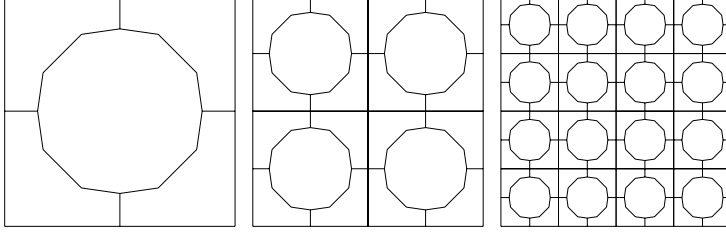


FIG. 7.2. The polygonal meshes consisting of dodecagons and heptagons are employed in Test Example 1.

7.1. Test Example 1. We carefully choose an exact solution which has a jumping stress at the interface,

$$(7.3) \quad \mathbf{u} = \begin{pmatrix} -\mu^{-1} \sin(\pi x) \cos(2\pi x) \sin(\pi y) \cos(2\pi y) \\ \mu^{-1} \sin(\pi x) \cos(2\pi x) \sin(\pi y) \cos(2\pi y) \end{pmatrix}.$$

The load function is computed using the exact solution (7.3) and the elasticity interface problem (1.1); i.e.,

$$(7.4) \quad \mathbf{f} = \left\{ \begin{array}{l} \frac{\pi^2}{2} \left(36 \cos^3 \pi x \cos^3 \pi y (2\lambda_0 + 1) \right. \\ \quad + 36 \cos^2 \pi x \sin \pi y \cos^2 \pi y \sin \pi x (2\lambda_0 + 3) \\ \quad - 30 \cos^3 \pi x \cos \pi y (2\lambda_0 + 1) - 2 \cos^2 \pi x \sin \pi y \sin \pi x (18\lambda_0 + 23) \\ \quad - 30 \cos \pi x \cos^3 \pi y (2\lambda_0 + 1) - 2 \sin \pi x \sin \pi y^2 \cos \pi y (10\lambda_0 + 19) \\ \quad \left. + 25 \cos \pi x \cos \pi y (2\lambda_0 + 1) + 5 \sin \pi x \sin \pi y (2\lambda_0 + 3) \right), \\ 4\pi^2 \sin \pi x \sin \pi y (\cos^2 \pi x - \cos^2 \pi y) (2\lambda_0 + 1) \\ \frac{\pi^2}{2} \left(36 \cos^3 \pi x \cos^3 \pi y (2\lambda_0 + 1) \right. \\ \quad + 36 \cos^2 \pi x \sin \pi y \cos^2 \pi y \sin \pi x (2\lambda_0 + 3) \\ \quad - 30 \cos^3 \pi x \cos \pi y (2\lambda_0 + 1) - 2 \cos^2 \pi x \sin \pi y \sin \pi x (18\lambda_0 + 23) \\ \quad - 30 \cos \pi x \cos^3 \pi y (2\lambda_0 + 1) - 2 \sin \pi x \sin \pi y^2 \cos \pi y (10\lambda_0 + 19) \\ \quad \left. + 25 \cos \pi x \cos \pi y (2\lambda_0 + 1) + 5 \sin \pi x \sin \pi y (2\lambda_0 + 3) \right). \end{array} \right\}$$

Note that the load function \mathbf{f} is independent of coefficient jumps. It would ensure a non-smooth solution. The exact solution $\mathbf{u}(x, y)$ with $\mu_0 = 10$ and $\lambda_0 = 10$ is demonstrated in Figure 7.1. The patterned polygonal meshes consisting of dodecagons and heptagons shown in Figure 7.2 are employed in the computation. A weak finite element space, based on the lowest order $k = 1$; i.e.,

$$W_h = \{ \{ \mathbf{v}_0, \mathbf{v}_b \} : \mathbf{v}_0|_T \in [P_1(T)]^2, \mathbf{v}_b|_T \in P_{RM}(e), \forall T \in \mathcal{T}_h \},$$

is used in computing this example. The corresponding element is named P^1 WG element. Table 7.1 lists the errors in the discrete norm for \mathbf{u}_h and in the L^2 norm for \mathbf{u}_0 , for the P^1 WG element in various jump coefficient cases. We have observed from Table 7.1 that our WG method (3.3) for the elasticity interface problem (1.1) converges at the optimal order of error estimate in the discrete norm for \mathbf{u}_h independent of jump

coefficients, which is consistent with what the theory expects. Furthermore, we have also observed our WG method converges at the optimal order of error estimate for \mathbf{u}_0 in the L^2 norm independent of jump coefficients.

TABLE 7.1
Error profile of P_1 WG on polygonal meshes shown in Figure 7.2 for (7.3).

level	$\ Q_0 u - u_0\ _0$	rate	$\ Q_h u - u_h\ $	rate
by the P_1 WG element ($\mu_0 = 1, \lambda_0 = 1$)				
4	0.170E-01	1.9	0.144E+01	1.0
5	0.433E-02	2.0	0.722E+00	1.0
6	0.109E-02	2.0	0.361E+00	1.0
7	0.272E-03	2.0	0.181E+00	1.0
by the P_1 WG element ($\mu_0 = 10^2, \lambda_0 = 10^{-2}$)				
4	0.108E-01	1.9	0.785E+00	0.9
5	0.275E-02	2.0	0.395E+00	1.0
6	0.689E-03	2.0	0.198E+00	1.0
7	0.172E-03	2.0	0.989E-01	1.0
by the P_1 WG element ($\mu_0 = 10^{-1}, \lambda_0 = 10$)				
4	0.106E+00	2.0	0.747E+01	1.0
5	0.291E-01	1.9	0.375E+01	1.0
6	0.766E-02	1.9	0.188E+01	1.0
7	0.196E-02	2.0	0.943E+00	1.0

7.2. Test Example 2. To take advantage of superconvergence of weak Galerkin finite elements, and to show its order-two superconvergence ([1, 16, 30, 31]), the exact solution of (7.1) is chosen to be a piecewise polynomial of degree 5 as follows

$$(7.5) \quad \mathbf{u} = \begin{pmatrix} -\mu^{-1}y(4y-1)(4y-3)(4x-1)(4x-3) \\ \mu^{-1}x(4y-1)(4y-3)(4x-1)(4x-3) \end{pmatrix}.$$

In addition, the stabilizer $s(\cdot, \cdot)$ in the WG algorithm (3.3) is dropped in order to achieve the superconvergence. The load function \mathbf{f} is computed using the exact solution \mathbf{u} in (7.5) and the elasticity interface equation (7.1). Again, the load \mathbf{f} is smooth which implies a non-smooth solution \mathbf{u} .

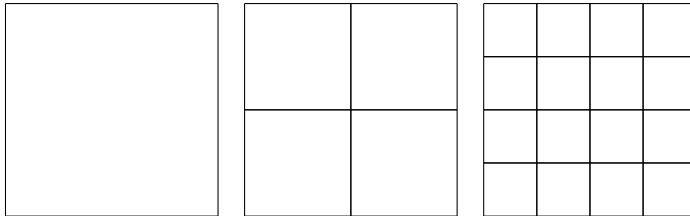


FIG. 7.3. The first three rectangular grids used in the computation of Table 7.2.

The uniform rectangular meshes shown in Figure 7.3 are employed. The numerical results of P_2 ($k = 2$) and P_3 ($k = 3$) WG finite elements are listed in Table 7.2. We can see from Table 7.2 that instead of 3rd order and 2nd order of convergence in the L^2 norm and the discrete norm for P_2 finite element solutions, we have 5th order and

and 4th order of superconvergence in the L^2 norm and the discrete norm respectively. Even though the exact solution \mathbf{u} is a piecewise P_5 polynomial, the P_3 WG finite element solution \mathbf{u}_h is exactly $Q_h\mathbf{u}$, if no rounding errors exist. These results are listed in Table 7.2 to see how computer round-off errors behave.

TABLE 7.2
Error profile on rectangular grids (Figure 7.3) for (7.5).

level	$\ Q_h u - u_h\ _0$	rate	$\ Q_h u - u_h\ $	rate
by the P_2 WG element ($\mu_0 = 1, \lambda_0 = 1$)				
3	0.117E-01	5.0	0.507E+00	4.0
4	0.366E-03	5.0	0.320E-01	4.0
5	0.116E-04	5.0	0.209E-02	3.9
6	0.389E-06	4.9	0.150E-03	3.9
by the P_3 WG element ($\mu_0 = 1, \lambda_0 = 1$)				
3	0.128E-12	0.0	0.199E-11	0.0
4	0.519E-12	0.0	0.677E-11	0.0
5	0.235E-11	0.0	0.248E-10	0.0
by the P_2 WG element ($\mu_0 = 10^2, \lambda_0 = 10^{-2}$)				
3	0.101E-01	5.2	0.366E+00	4.2
4	0.314E-03	5.0	0.229E-01	4.0
5	0.982E-05	5.0	0.143E-02	4.0
6	0.307E-06	5.0	0.893E-04	4.0
by the P_3 WG element ($\mu_0 = 10^2, \lambda_0 = 10^{-2}$)				
3	0.847E-13	0.0	0.157E-11	0.0
4	0.407E-12	0.0	0.613E-11	0.0
5	0.180E-11	0.0	0.236E-10	0.0

7.3. Test Example 3. In this test, we shall compute the numerical solutions arising from WG scheme (3.3) for the elasticity interface model problem (7.1) when the exact solution is unknown. That is, we choose a smooth load \mathbf{f} directly. Find $\mathbf{u} \in H_0^1(\Omega)^2$ such that

$$(7.6) \quad (2\mu\boldsymbol{\epsilon}(\mathbf{u}), \boldsymbol{\epsilon}(\mathbf{v})) + (\lambda\nabla \cdot \mathbf{u}, \nabla \cdot \mathbf{v}) = \left(\begin{pmatrix} 0 \\ 1 \end{pmatrix}, \mathbf{v} \right) \quad \forall \mathbf{v} \in H_0^1(\Omega)^2,$$

where $\Omega = (0, 1)^2$, μ and λ are defined in (7.2). The rectangular meshes shown in Figure 7.3 are employed. The P_4 ($k=4$) weak Galerkin solution on the 4th rectangular grids shown as in Figure 7.3, is plotted in Figure 7.4, with $\mu_0 = 1$ and $\lambda_0 = 1$.

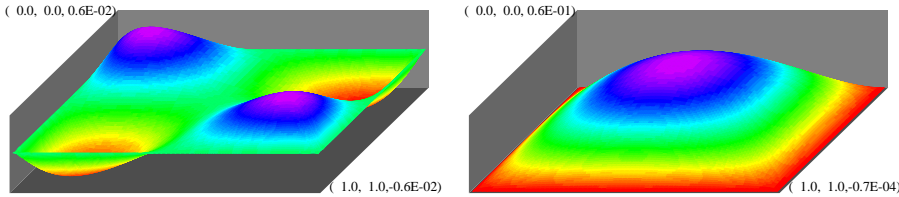


FIG. 7.4. The P_4 WG solution ($\mu_0 = 1, \lambda_0 = 1$) on the 4th rectangular grids (cf. Figure 7.3).

We plot the solutions of the other two interface cases in Figures 7.5 and 7.6. In these two cases, due to re-entrant interface corners, the solutions are not smooth near these 4 points. We can observe from Figures 7.5 and 7.6 that the large jumps of the discontinuous finite element solutions arise at the four points. Additionally we plot the deformation of the linear elasticity for the two cases, under the unit upward load, in Figure 7.7. On the left, as we have a hard material in the center, the deformation is almost identical in the center square. As we have the whole material highly compressible, the deformation is almost one directional, i.e., the deformation field is irrotational. On the right, as we have the softer material in the center, the deformation is almost limited inside the center square. Here we have nearly incompressible material everywhere. The deformation is nearly solenoidal, i.e., the deformation almost circles around inside the center square.

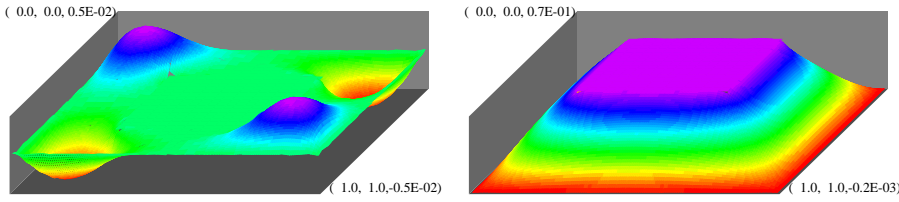


FIG. 7.5. The P_4 WG solution ($\mu_0 = 10^3$, $\lambda_0 = 10^{-3}$) on the 4th rectangular grid (cf. Figure 7.3).

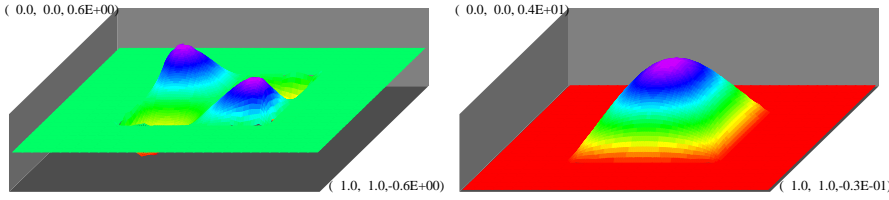


FIG. 7.6. The P_4 WG solution ($\mu_0 = 10^{-3}$, $\lambda_0 = 10^3$) on the 4th rectangular grid (cf. Figure 7.3).

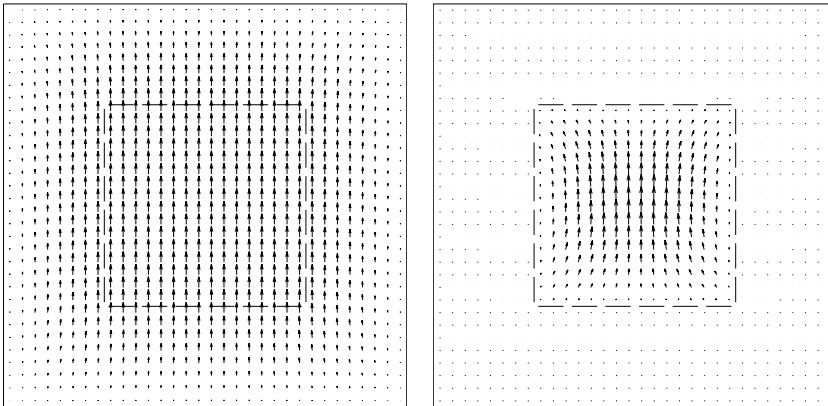


FIG. 7.7. The deformation of a linear elasticity under the unit upward load. Left: $\mu_0 = 10^3$, $\lambda_0 = 10^{-3}$. Right: $\mu_0 = 10^{-3}$, $\lambda_0 = 10^3$.

REFERENCES

- [1] A. Al-Taweel, X. Wang X. Ye and S. Zhang, *A stabilizer free weak Galerkin finite element method with supercloseness of order two*, Numer. Methods Partial Differential Equations 37 (2021), no. 2, 1012–1029.
- [2] A. Anandarajah, *Computational Methods in Elasticity and Plasticity: Solids and Porous Media*, Springer, 2010.
- [3] R. Becker, E. Burman, P. Hansbo, *A Nitsche extended finite element method for incompressible elasticity with discontinuous modulus of elasticity*, Comput. Methods Appl. Mech. Engrg. 198(2009)3352–3360.
- [4] Y.Z.Chang, *Adaptive finite element method for elasticity interface problems*, J.Comput.Math.30(2012)629–642.
- [5] G. Dvorak, *Micromechanics of Composite Materials*, Springer, 2013.
- [6] Y.Gong, Z.L.Li, *Immersed interface finite element methods for elasticity inter face problems with non-homogeneous jump conditions*, Numer.Math.Theory Methods Appl.3(2010)23–39.
- [7] T.P.Fries,T.Belyschko, *The extended/generalized finite element method:an overview of the method and its applications*, Internat. J. Numer. Methods Engrg. 84(2010)253–304.
- [8] A.Hansbo, P.Hansbo, *An unfitted finite element method*, Comput. Methods Appl. Mech. Engrg.191(2002)5537–5552.
- [9] S. Hou, Z. Li, L. Wang, W. Wang, *A numerical method for solving elasticity equations with sharp-edged interfaces*, Commun. Comput. Phys. 12 (2012) 595–612.
- [10] T. Lin, D.W. Sheen, X. Zhang, *A locking-free immersed finite element method for planar elasticity interface problems*, J. Comput. Phys. 247 (2013) 228–247.
- [11] Z.L.Li, X.Z.Yang, *An immersed fem for elasticity equations with interfaces*, AMS Contemp. Math.383(2005)285–298.
- [12] T. Lin, X. Zhang, *Linear and bilinear immersed finite elements for planar elasticity interface problems*, J. Comput. Appl. Math. 236 (2012) 4681–4699.
- [13] R.J.LeVeque,Z.L.Li, *The immersed inter face method for elliptic equations with discontinuous coefficients and singular sources*, SIAM J.Numer.Anal.31(1994)1019–1044.
- [14] J.Mergheim, *Computational modeling of strong and weak discontinuities (Ph.D.thesis)*, Technical University of Kaisers lautern,2006.
- [15] M. Michaeli,F. Assous, A. Golubchik, *An nitche type method for stress fields calculation in dissimilar material with inter facec rack*, Appl. Numer.Math.67(2013)187–203.
- [16] L. Mu, X. Ye and S. Zhang, *A stabilizer-free, pressure-robust, and superconvergence weak Galerkin finite element method for the Stokes equations on polytopal mesh*, SIAM J. Sci. Comput. 43 (2021), no. 4, A2614–A2637.
- [17] N. Sukumar, D.L.Chopp, N.Moes,T.Belytschko, *Modeling holes and inclusions by level sets in the extended finite-element method*, Comput. Methods Appl. Mech. Engrg. 190(2001)6180–6200.
- [18] P.M.Shearer, *Introduction to Seismology*, Cambridge University Press,1999.
- [19] M. Stolarska, D.L. Chopp, N. Moes, T. Belytschko, *Modelling crack growth by level sets in the extended finite element method*, Internat. J. Numer. Methods Engrg.51(2001)943–960.
- [20] M. Theillard, L.F.Djodjom, J.L.Vie, F. Gibou, *A second-order sharp numerical method for solving the linear elasticity equations on irregular domains and adaptive grids—application to shape optimization*, J.Comput. Phys. 233(2013)430–448.
- [21] G.W.Weil, *Differential geometry based multiscale models*,Bull.Math.Biol.72(2010)1562–1622.
- [22] G. W.Weil, *Multiscale,multi physics and multi domain models I:basic theory*, J.Theor. Comput. Chem.12(8)(2013)1341006.
- [23] C.T. Wu, Y. Guo, E. Askari, *Numerical modeling of composite solids using an immersed mesh-free Galerkin method*, Composites B 45 (2013) 1397–1413.
- [24] C. Wang, J. Wang, R. Wang and R. Zhang, *A Locking-Free Weak Galerkin Finite Element Method for Elasticity Problems in the Primal Formulation*, Journal of Computational and Applied Mathematics, Vol. 307, pp. 346–366, 2016.
- [25] J. WANG AND X. YE, *A weak Galerkin mixed finite element method for second-order elliptic problems*, Math. Comp., vol. 83, pp. 2101–2126, 2014.
- [26] X.S.Wang, L.T.Zhang, W.K.Liu, *On computational issues of immersed finite element methods*, J.Comput.Phys.228(2009)2535–2551.
- [27] H.Xie, Z.L.Li, Z.H.Qiao, *A finite element method for elasticity interface problems with locally modified triangulations*, Int.J.Numer.Anal.Model.8(2011)189–200.
- [28] K.L.Xia, K.Opron, G.W.Weil, *Multiscale multiphysics and multidomain models -flexibility and rigidity*,J.Chem.Phys.139(2013)194109.

- [29] X.Z.Yang, B.Li, Z.L.Li, *The immersed interface method for elasticity problems with interface*, Dyn. Contin. Discrete Impuls. Syst. Ser. A Math. Anal. 10(2003)783–808.
- [30] X. Ye and S. Zhang, *A P_{k+2} polynomial lifting operator on polygons and polyhedrons*, Appl. Math. Lett. 116 (2021), Paper No. 107033, 6 pp.
- [31] X. Ye and S. Zhang, *A stabilizer free WG Method for the Stokes Equations with order two superconvergence on polytopal mesh*, Electron. Res. Arch. 29 (2021), no. 6, 3609–3627.